This case report is unusual and novel for two reasons. First, DBS-related complications occurring 72 h after DBS surgery are quite rare events: surgical complications commonly manifest during surgery or in the ensuing hours and are already demonstrated by postoperative imaging (3–4 h after surgery) (Fenoy and Simpson, 2014). Second, though a previous report (Novak et al., 2006) has described abnormal intraoperative single unit recordings in DBS-related ischemia, none have reported LFP changes associated with a brain lesion or suggesting a DBS-related complication. We conjecture that in our patient a stunning phase causing LFP recording abnormalities preceded a phase characterized by further LFP changes and clinical manifestations. As well as a small hemorrhagic hyperdensity, the CT scan identified a slight hypodensity in the right cerebral peduncle and midbrain and extending through the pons that probably reflected edema because it caused only mild neurological deficits and was fully reversible 30 days after the event.

A technically important finding was that as a variable for diagnosing a possible DBS complication, LFP electrode impedance proved less sensitive than LFP amplitude. In fact, in the first recording session – one day before the patient's hemiparesis began – electrode impedance was only slightly lower in the right than in the left STN. Conversely, the LFP recordings already showed reduced amplitude in the right side unaccompanied by the typical spectral oscillatory pattern. We could hypothesize that, in the early stunning phase, neuronal apraxia impairs neuronal oscillatory activity thus leading to abnormal LFP recordings. Afterwards, brain edema and bleeding alter also tissue conductivity and ultimately reduce impedance.

In conclusion, our case report underlines that early asymmetry in LFP recordings after DBS surgery should alert neurologists to possible DBS-related complications, occurring in proximity to the electrode's apex. Even though CT scan remains quickest and the most useful method for detecting the hemorrhage, our study suggest that LFP recording could be useful not only for scientific purpose but also to detect some kinds of preclinical surgical complications (in particular the ones occurring near the electrode's apex). Being a quick and safe method it can be repeated several times a day, if available, especially in patients at risk as patients with comorbidities or with advanced age.

Acknowledgement

This study was supported by Fondazione IRCCS Ospedale Maggiore Policlinico, Mangiagalli, Regina Elena (Milan, Italy), Università degli Studi di Milano (Italy), Ministero della Sanità (Italy), Ministero dell'Università e della Ricerca Scientifica e Tecnologica (Italy).

Conflict of Interest: None of the authors have potential conflicts of interest to be disclosed.

References

Chen CC, Pogosyan A, Zrinzo LU, Tisch S, Limousin P, Ashkan K, et al. Intra-operative recordings of local field potentials can help localize the subthalamic nucleus in Parkinson's disease surgery. Exp Neurol 2006;198:214–21.

Fenoy AJ, Simpson Jr RK. Risks of common complications in deep brain stimulation surgery: management and avoidance. J Neurosurg 2014;120:132–9.

Giannicola G, Marceglia S, Rossi L, Mrakic-Sposta S, Rampini P, Tamma F, et al. The effects of levodopa and ongoing deep brain stimulation on subthalamic beta oscillations in Parkinson's disease. Exp Neurol 2010;226:120–7.

Novak KE, Nenonene EK, Bernstein LP, Vergenz S, Medalle G, Prager JM, et al. Two cases of ischemia associated with subthalamic nucleus stimulator implantation for advanced Parkinson's disease. Mov Disord 2006;21:1477–83.

Rampini PM, Locatelli M, Alimehmeti R, Tamma F, Caputo E, Priori A, et al. Multiple sequential image-fusion and direct MRI localisation of the subthalamic nucleus for deep brain stimulation. J Neurosurg Sci 2003;47:33–9.

Francesca Cortese[1]
Fondazione IRCCS Ca' Granda Ospedale Maggiore Policlinico, Milan, Italy
Università degli Studi di Milano, Milan, Italy
Dipartimento di Medicina, Scienze Chirurgiche e Biotecnologie, Univerisità la Sapienza di Roma, polo pontino, Latina, Italy

Manuela Rosa[1]
Fondazione IRCCS Ca' Granda Ospedale Maggiore Policlinico, Milan, Italy
Università degli Studi di Milano, Milan, Italy

Mattia Arlotti
Fondazione IRCCS Ca' Granda Ospedale Maggiore Policlinico, Milan, Italy

Filippo Cogiamanian
Fondazione IRCCS Ca' Granda Ospedale Maggiore Policlinico, Milan, Italy

Gianluca Ardolino
Fondazione IRCCS Ca' Granda Ospedale Maggiore Policlinico, Milan, Italy

Paolo Rampini
Fondazione IRCCS Ca' Granda Ospedale Maggiore Policlinico, Milan, Italy

Giorgio Carrabba
Fondazione IRCCS Ca' Granda Ospedale Maggiore Policlinico, Milan, Italy

Marco Locatelli
Fondazione IRCCS Ca' Granda Ospedale Maggiore Policlinico, Milan, Italy

Vincenzo Levi
Università degli Studi di Milano, Milan, Italy

Alberto Priori *
Fondazione IRCCS Ca' Granda Ospedale Maggiore Policlinico, Milan, Italy
Università degli Studi di Milano, Milan, Italy

* Corresponding author at: Università degli Studi di Milano, Centro Clinico per la Neurostimolazione, le Neurotecnologie ed i Disordini del Movimento, Fondazione IRCCS, Ca' Granda Ospedale Maggiore Policlinico, Via Francesco Sforza 35, Milano 20122, Italy.
E-mail address: alberto.priori@unimi.it (A. Priori)

Available online 6 September 2014

[1] The first two authors are in alphabetical order.

http://dx.doi.org/10.1016/j.clinph.2014.08.014

Unexpected nerve neuroimaging findings in Friedreich's ataxia

Friedreich's ataxia (FRDA) is the most common autosomic recessive ataxia, caused by homozygous expansion of guanine–adenine–adenine (GAA) trinucleotide repeat in the frataxin gene leading to decreased expression of mitochondrial protein frataxin.

The major neurological features are ataxia, dysarthria, areflexia, but sensory axonal neuropathy does also occur. Systemic symptoms (cardiomyopathy, scoliosis, diabetes mellitus) often coexist. Neurological phenotype is due to the involvement of dorsal root ganglia, sensory peripheral nerves, corticospinal tracts and dentate nuclei. Neurophysiological studies show severe reduction of sensory nerves action potential amplitude with preservation of nerve conduction velocities, consistent with sensory axonal damage. The neurophysiological abnormalities correlate with the size of GAA repeat expansion and with neuropathological findings (Santoro et al., 1999).

Symptoms due to ataxia usually exceed those from sensory axonal neuropathy that are likely underestimated and contribute to patients' disability.

Table 1
Nerve conduction studies.

Nerve	Stimulation site	DL (ms)	CV (m/s)	Amplitude (cMAP = mV SAP = μV)	F latency (ms)
L median (m)	Wrist	3.40		11	29
	Elbow		60	10	
	Axilla		71	10	
R median (m)	Wrist	3.08		12	30
	Elbow		53	8	
	Axilla		57	8	
R ulnar (m)	Wrist	2.67		14	27
	BE		54	13	
	AE		57	13	
	Axilla		62	13	
R tibial (m)	Ankle	4.12		11	47
	PF		46	9	
L peroneal (m)	Ankle	4.80		3	48
	AFH		49	3	
L median (s)	1st finger		NR	NR	
	3rd finger		NR	NR	
R ulnar (s)	5th finger		57	1	
R radial (s)	1st finger		NR	NR	
L radial (s)	1st finger		NR	NR	
R lat ant cut (s)	AF		NR	NR	
L lat ant cut (s)	AF		NR	NR	
R sural (s)	Mild calf		46	2	
L sural (s)	Mild calf		NR	NR	

DL: distal latency; CV: conduction velocity; cMAP: compound motor action potential; SAP: sensory action potential; BE: below elbow; AE: above elbow; PF: popliteal fossa; AFH: above fibular head; Lat ant cut: lateral antebrachial cutaneous; AF: antecubital fossa; NR: no response. R: right; L: left; m: motor; s: sensory.
Normal values: median nerve DL ⩽ 3,5 ms; SCV ⩾ 48 m/s; SAP ⩾ 15 μV; MCV ⩾ 50 m/s; cMAP ⩾ 6 mV; ulnar nerve DL ⩽ 3,1 ms; SCV ⩾ 48 m/s; SAP ⩾ 10 μV; MCV ⩾ 50 m/s; cMAP ⩾ 4 mV; radial nerve SCV ⩾ 40 m/s; SAP ⩾ 10 μV; peroneal nerve DL ⩽ 5,5 ms; MCV ⩾ 40 m/s; cMAP ⩾ 3 mV; tibial nerve DL ⩽ 6,0 ms; MCV ⩾ 40 m/s; cMAP ⩾ 3 mV; sural nerve SCV ⩾ 50 m/s; SAP ⩾ 5 μV; lateral antebrachial cutaneous nerve SCV ⩾ 55 m/s; SAP ⩾ 15 μV; F-wave median/ulnar < 32 ms; peroneal/tibial <56 ms.

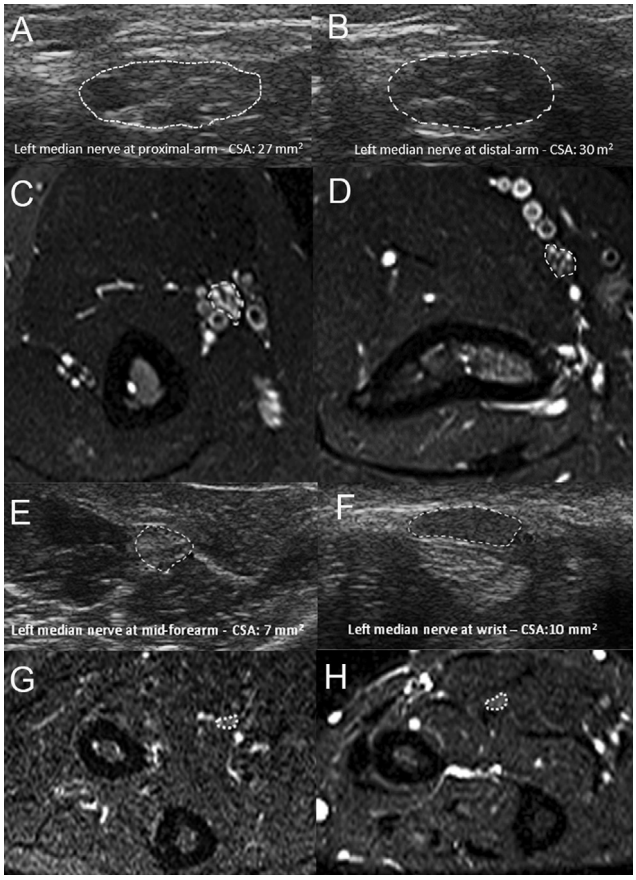

Fig. 1. Left median nerve: comparison of US and MRN findings at proximal (A and C) and distal (B and D) arm, mid-forearm (E and G) and wrist (F and H). US shows CSA enlargement with heterogeneous hypo- and hyper-echoic hypertrophic fascicles of the median nerve at proximal (A) and distal (B) arm (normal values ⩽ 11 mm^2). At MRN the median nerve is enlarged and markedly hyperintense, with fascicular hypertrophy both in proximal (C) and distal (D) sections. The CSA, measured approximately at the same levels by the two imaging modalities, is comparable. According to US (E and F) and MRN (G and H) examinations the median nerve is back to a normal appearance at mid-forearm and wrist.